C_α/C_c Concept Applied to Compression of Peat[a]

Discussion by G. Mesri,[4] Member, ASCE, T. D. Stark,[5] Associate Member, ASCE, and C. S. Chen[6]

The statement in Mesri and Castro (1987) reads: "For a variety of natural materials, including peats, organic silts, highly sensitive clays, shales, as well as granular materials, the values of C_α/C_c are in the remarkably narrow range of 0.02–0.10. The authors misinterpret this statement and credit Mesri and Castro (1987) for reporting a C_α/C_c range of 0.02–0.10 for peats. Actually, Mesri and Castro (1987) further suggested C_α/C_c values of 0.04 ± 0.01 for soft clays and 0.05 ± 0.01 for highly organic plastic clays. Values of C_α/C_c in the range of 0.015–0.03 pertain to granular soils (Mesri et al. 1990), and existing reliable data for peats indicate C_α/C_a values commonly in the range of 0.06–0.07 [e.g., Mesri (1986)]. Therefore, the range of values of C_α/C_c for peat from authors' tests and interpretation is quite unreasonable.

The authors incorrectly paired C_α data in recompression with C_c data from the compression range. The C_c values of 5–9 1/2 in compression in Fig. 5 substantially overestimate the C_c in recompression that controlled the initial part of the secondary compression curve and thus C_α. Note that in the C_α/C_c concept, C_c is used to denote slopes of $e - \log \sigma'_v$ in recompression as well as in compression. When only a single test is used to define C_α/C_c for a soil, it is prudent to make secondary compression observations only at a few pressure increments, separated from each other by increments that are maintained up to the end of primary consolidation, so that the C_α and C_c pair are readily defined.

It is quite unfortunate that the authors see a need to complicate secondary compression behavior of peat by introducing concepts such as "tertiary creep." A secondary compression curve on which C_α strongly increases with time, has been repeatedly observed for soft clays [e.g., Fig. 3 of Mesri and Castro (1987) or Figs. 4(*c*) and 7(*d*) of Mesri (1987)]. The authors have taken continuous secondary compression curves such as those in Figs. 1 and 7, and arbitrarily divided them into two parts. Secondary compression behavior such as those in Figs. 1 and 7 is expected and has been repeatedly observed whenever a pressure increment ends near the in situ preconsolidation pressure, or near a critical pressure developed in laboratory by such mechanisms as secondary compression. A considerable increase in C_c from recompression to the compression range results in the significant increase in C_α with time. This is predicted by the C_α/C_c law of compressibility (Mesri 1987).

The authors have provided the writers with tabulations of compression with time for the pressure increments of oedometer tests 5 and 7. For all pressure increments of both tests, a plot of compression against log time indicates a significant increase in secondary compression index $C_\alpha = \Delta e/\Delta \log t$ with time. An example is shown in Fig. 8 in which data on C_α are obtained by approximating the continuous secondary compression curve by three linear segments. In order to explain the behavior of C_α with time and to obtain data on the corresponding values of C_c, axial strains at the end

[a]August, 1992, Vol. 118, No. 8, by Patrick J. Fox, Tuncer B. Edil, and Li-Tus Lan (Paper 2013).

[4]Prof., Dept. of Civ. Engrg., Univ. of Illinois, Newmark Civ. Engrg. Lab. MC-250, 205 N. Mathews Ave., Urbana, IL 61801.

[5]Asst. Prof., Dept. of Civ. Engrg., Univ. of Illinois, Urbana, IL.

[6]Grad. Student, Univ. of Illinois, Urbana, IL.

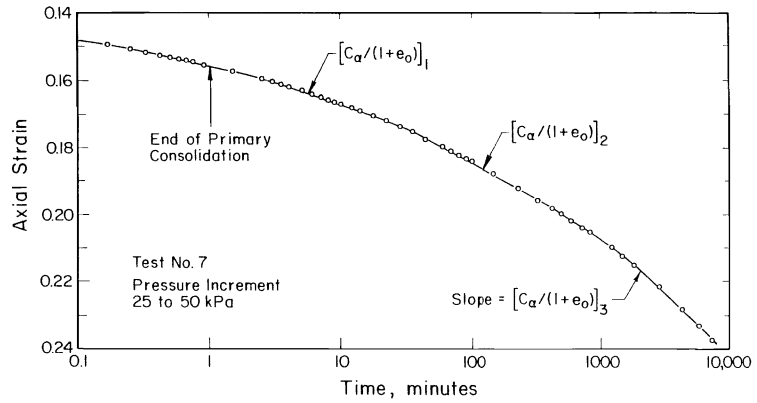

FIG. 8. Secondary Compression of Peat Showing Increase in C_α with Time

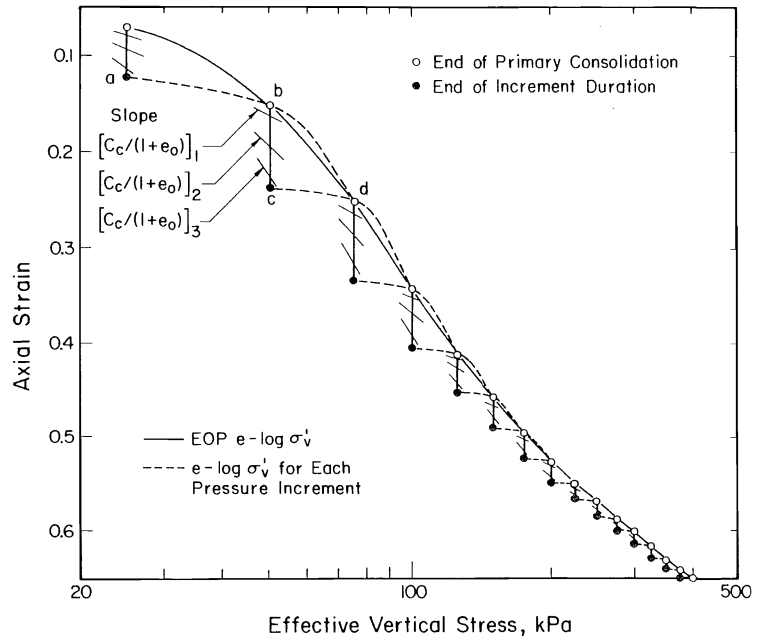

FIG. 9. Primary and Secondary Compression for Each Pressure Increment of Test 7

of primary consolidation and end of pressure increment duration were plotted against log effective vertical stress. Fig. 9 shows the resulting relationship for test 7, and provides an explanation for the observed increase in C_α with time. In both tests 5 and 7, since significant secondary compression was allowed under all pressure increments, every pressure increment started on a recompression curve and barely reached the end-of-primary (EOP) compression curve. For example, the pressure increment from 25 to 50 kPa

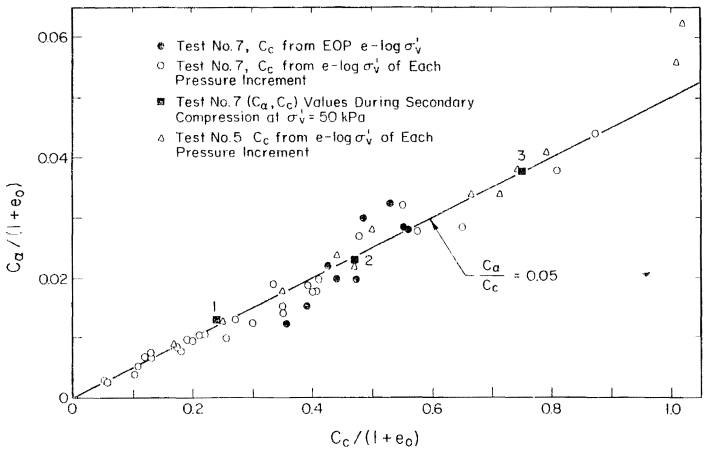

FIG. 10. Secondary Compression Data for All Pressure Increments and Full Increment Durations of Tests 5 and 7

started at point a, primary compression took place on the recompression curve a to b, and secondary compression followed from b to c.

The values of C_c corresponding to the C_α along b-c can be estimated from the shape of the dashed recompression to compression curve a-b-d. This procedure has been previously explained in Fig. 4 of Mesri and Godlewski (1977) and in Fig. 6 of Mesri (1986). In the present case, the exact shapes of curves such as a-b-d were not measured; however, they can be estimated with the aid of EOP e-log σ'_v curve. In fact, for pressure increments at values of σ'_v than about 150 kPa, the compression part of the e-log σ'_v curves such as a-b-d merge with the EOP e-log σ'_v defined by all pressure increments. Therefore, for these pressure increments, secondary compression index from the last segment of e-log t, i.e., $C_{\alpha 3}$, was paired with C_{c3}, which was determined at the same axial strain from the EOP e-log σ'_v curve. These data points that are plotted as the solid circles in Fig. 10, lead to a $C_\alpha/C_c = 0.05$. For the rest of the pressure increments and at all times during secondary compression, the values of C_c were computed from $C_c = C_\alpha/0.05$. These values of C_c, which are shown in Fig. 9, were used as a guide for sketching the dashed e-log σ'_v curves, such as a-b-d, for each pressure increment. The values of C_α, together with C_c at the same axial strain from the dashed e-log σ'_v curve of each pressure increment, are plotted for both tests 5 and 7 in Fig. 10. As an example, note the three pairs of values of (C_α, C_c) in Fig. 10, during secondary compression from b to c at $\sigma'_v = 50$ kPa in Fig. 9. In summary, the dashed e-log σ'_v curves in Fig. 9, which are quite reasonable, correspond to a single value of C_α/C_c.

The only unusual result of tests 5 and 7 is the relatively small value of $C_\alpha/C_c = 0.05$ for this particular peat as compared to a typical value of near 0.06 for other peats. In conclusion, a proper interpretation of authors' test results supports the C_α/C_c concept, and indicates that the value of C_α/C_c for some peats may be as low as 0.05. These, together with previous reliable data, suggest C_α/C_c values of 0.06 ± 0.01 for peats.

APPENDIX. REFERENCES

Mesri, G. (1986). "Discussion of 'Post construction settlement of an expressway built on peat by precompression.'" *Can. Geotech. J.*, 23, 3, 403–407.

Mesri, G. (1987). "Fourth law of soil mechanics: A law of compressibility." *Proc. Int. Symp. on Geotech. Engrg. Soft Soils*, 2, 179–187.
Mesri, G., Feng, T. W., and Benak, J. M. (1990). "Postconstruction penetration resistance of clean sands." *J. Geotech. Engrg.*, ASCE, 116(7), 1095–1115.

Closure by Patrick J. Fox,[7] Associate Member, ASCE, Tuncer B. Edil,[8] Member, ASCE and Li-Tus Lan[9]

The writers thank Mesri, Stark, and Chen for their comments and welcome an open dialogue on the applicability of the C_α/C_c concept to unusual soils such as peat.

The discussers take issue with the term "tertiary compression" as used by the writers to designate the increase of C_α with time on an e-log t plot. In principle, "tertiary compression" was first recognized as a "type III" secondary compression curve by Marsal et al. (1950). Leonards and Girault (1961) and Lo (1961) also discuss this shape and note that it occurs for all soils under a small load-increment-ratio (LIR). For Middleton peat, C_α increases with time for all load increments, not only those for small LIR. Thus, the term "tertiary compression" was used as a convenient means to distinguish between small C_α values that occur immediately after primary consolidation and the larger C_α values that invariably occur later in time. In Figs. 3, 4, 5, and 6, the term is used to demonstrate that the persistent tertiary compression for Middleton peat tends to worsen correlations between C_α and C_c. The writers do recognize that "tertiary compression" may be confused with the term "tertiary creep" used to designate a true increase in strain rate with time that ultimately leads to creep failure (Finnie and Heller 1959). No such increase in strain rate occurs during compression and the concave-down shape of the time-settlement curve results from the logarithmic time scale.

The discussers raise questions concerning the writers' interpretation of the C_α/C_c concept. The procedure used by the writers to compute C_α/C_c values is given in Fig. 1 of Mesri and Castro (1987). In particular, the discussers make the central assertion that, in both tests 5 and 7, "every pressure increment started on a recompression curve and barely reached the end-of-primary (EOP) compression curve." As a result, C_c values used by the writers (the solid curve in Fig. 9) are deemed unacceptable and the discussers state that the correct C_c values are given by the dashed "recompression" curves (abd) in Fig. 9. It is the writers' understanding that these dashed curves were prepared in the following manner:

1. Each dashed recompression curve was assumed to merge with the solid EOP curve at point d, especially for effective stress levels above 150 kPa.
2. For stress levels above 150 kPa, C_α from the last segment of each e-log t curve was paired with C_c given by the solid EOP curve at the same axial strain. These pairs are plotted as solid circles in Fig. 10. A line drawn through the solid circles and the origin gave $C_\alpha/C_c = 0.05$.
3. Using $C_\alpha/C_c = 0.05$ and known C_α values during creep, C_c values were calculated and used to draw the dashed recompression curves.

[7]Asst. Prof., School of Civil Engrg., Purdue Univ., West Lafayette, IN.
[8]Prof., Dept. of Civil and Envir. Engrg., Univ. of Wisconsin, Madison, WI.
[9]Supervisory Engr., Pacific Engineers & Constructors, Ltd., Taipei, Taiwan.

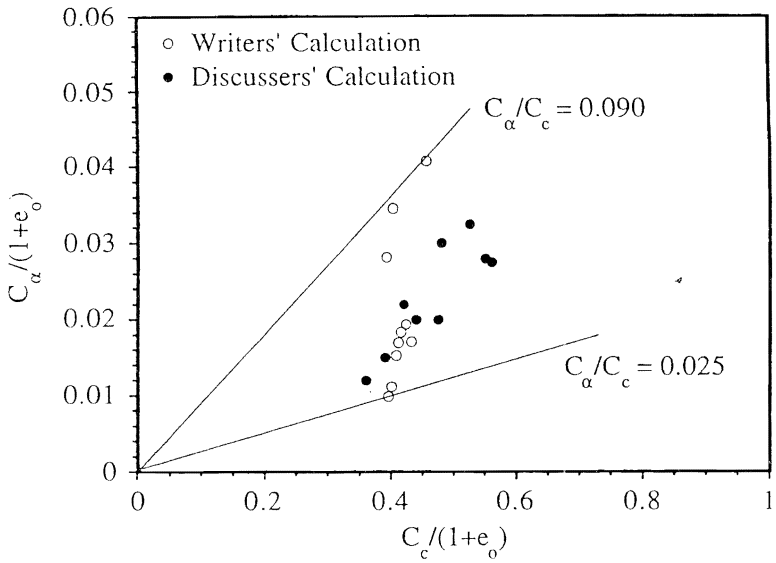

FIG. 11. C_α versus C_c Data for Test 7 at Stress Levels above 150 kPa

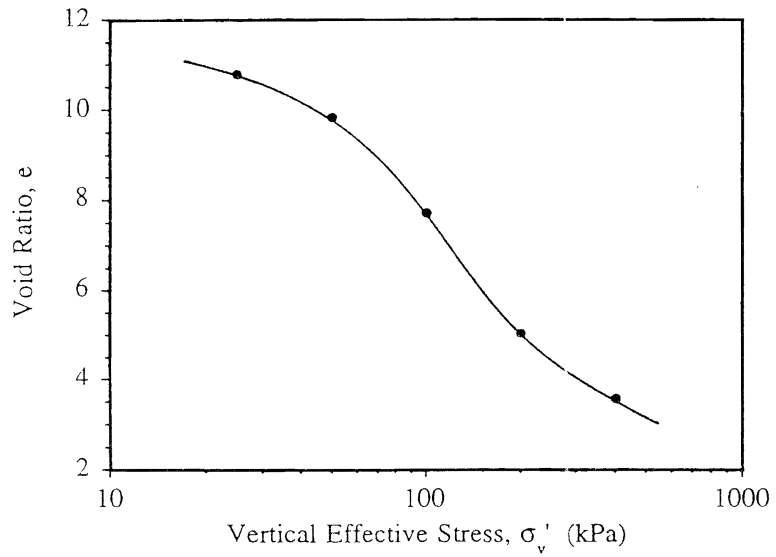

FIG. 12. EOP e-log σ_v' Curve for Test 6

Once the dashed curves were drawn in Fig. 9, they were used to back-calculate C_c values for corresponding C_α values at any given strain. The remainder of points plotted in Fig. 10 (i.e., those other than the solid circles) were computed in this fashion.

The solid circles in Fig. 10 give a range of C_α/C_c values from 0.034 to 0.062. Returning to the original data for test 7, the writers followed the

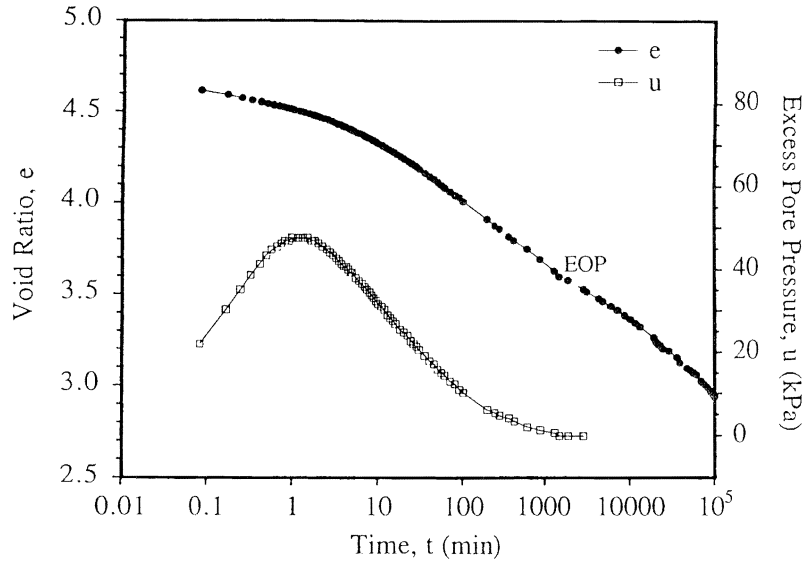

FIG. 13. e-log t Curve for Test 6 at 400 kPa

same procedure as just outlined and obtained C_α/C_c values ranging from 0.025 to 0.090. These two data sets are compared in Fig. 11. The solid circles of Fig. 11 are the same as those in Fig. 10 and the open circles were calculated by the writers. Considering this figure, it is difficult to accept the postulate that C_α/C_c is a constant for Middleton peat. As a result, there seems little basis for using $C_\alpha/C_c = 0.05$ to compute the remainder of data points in Fig. 10.

The writers can provide additional evidence that, for Middleton peat, the C_α/C_c ratio may not be a unique value. Fig. 12 shows the EOP compressibility curve for test 6 in which the vertical stress was doubled every five days. The last load, 400 kPa, remained on the specimen for 10 weeks. For tests on Middleton peat having LIR = 1, Edil et al. (1992) found no significant difference among EOP void ratios for load increment durations of EOP, two days, two weeks and 10 weeks. Therefore, Fig. 12 can be considered to be an appropriate EOP curve to calculate C_c values for analysis.

Fig. 13 shows the time-settlement curve for the 40-kPa increment of test 6. C_α increases during creep compression from 0.336 to 0.484. From Fig. 12, C_c would clearly be expected to *decrease* for the same load increment. If, however, C_c is approximated by a constant value of 3.85, C_α/C_c ranges from 0.087 to 0.126.

Middleton peat is a fibrous material with an organic content in excess of 90%. It has high permeability, high compressibility, and displays exaggerated creep effects compared to common inorganic soils. The writers recommend caution if the C_α/C_c concept is used for such materials.

APPENDIX. REFERENCES

Finnie, I., and Heller, W. P. (1959). *Creep of engineering materials*. McGraw-Hill, New York, N.Y.

Leonards, G. A., and Girault, P. (1961). "A study of the one-dimensional consolidation test." *Proc., 5th ICSMFE*, 1, 213–218.

Lo, K. Y. (1961). "Secondary compression of clays." *J. Soil Mech. and Found. Engrg. Div.*, ASCE, 87(4), 61–87.
Marsal, R. J., Sandoval, R., and Hiriart, F. (1950). "Curvas 'deformacion-tiempo' en las arcillas del valle de Mexico." *Ingenieria Civil*, Colegio de Ingenieros Civiles de Mexico, Ano II, V, VII–17 (in Spanish).

GENERALIZED CREEP AND STRESS RELAXATION MODEL FOR CLAYS[a]

Discussion by Victor N. Kaliakin,[2] Member, ASCE

The paper's major premise is the requirement of "at least two phenomenological models," one for creep and another for stress relaxation. Yet the author is apparently unaware of, or has ignored the body of work based on the concept of a bounding surface, and extended to include time-dependent behavior via an elastoplastic-viscoplastic formulation (Kaliakin and Dafalias 1990a, 1990b). Past results show this formulation capable of accurately simulating the time dependent behavior of cohesive soils without the need for separate models for creep, stress relaxation or any other behavioral aspect.

The general bounding surface formulation for isotropic soils is cast in the space of three invariants (I, J, α) of the effective stress tensor σ_{ij}. A section of the elliptical bounding surface is shown in Fig. 12. The parameter R ($R \geq 2.0$) defines the size of the surface. In the modified Cam Clay formulation, as in the author's model, R was fixed at 2.0. Past results indicate, however, that the ability to vary R improves numerical simulations.

The prominent feature of the bounding surface concept is the prediction of inelastic deformations for stress points (I, J) within or on the surface at a pace depending on the proximity of (I, J) to unique "image" points $(\bar{I}, \bar{J})$ on the surface, assigning by the mapping

$$\bar{I} = b(I - CI_0) + CI_0 \tag{48}$$

with $\bar{J} = bJ$ and $\bar{\alpha} = \alpha$. The variable b is determined in terms of the material state, I_0 quantifies the preconsolidation history (in the author's notation, $I_0 = 3p_c$), and C = a model parameter (Fig. 12). Unlike formulations that model gradual inelastic deformations using multiple surfaces (Hsieh et al. 1990), the present approach is conceptually straightforward and successfully predicts response at any overconsolidation ratio. As such, it improves upon deficiencies associated with Cam Clay based formulations.

The infinitesimal strain rate tensor is decomposed as

$$\dot{\varepsilon}_{ij} = \dot{\varepsilon}^e_{ij} + \dot{\varepsilon}^v_{ij} + \dot{\varepsilon}^p_{ij} \tag{49}$$

where the superscripts e, v, and p denote its elastic, viscoplastic and plastic components, respectively, and a dot indicates a material time derivative.

The rate $\dot{\varepsilon}^v_{ij}$ is a function of the "distance" between (I, J) and the boundary of an elastic domain (Perzyna 1966). The "normalized overstress"

[a]November, 1992, Vol. 118, No. 11, by R. I. Borja (Paper 2140).
[2]Asst. Prof., Univ. of Delaware, Newark, DE 19716.

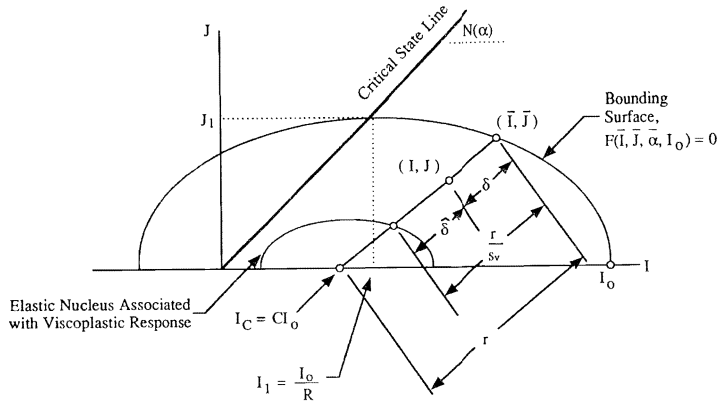

FIG. 12. Schematic Illustration of Radial Mapping Rule and of Bounding Surface in Stress Invariants Space

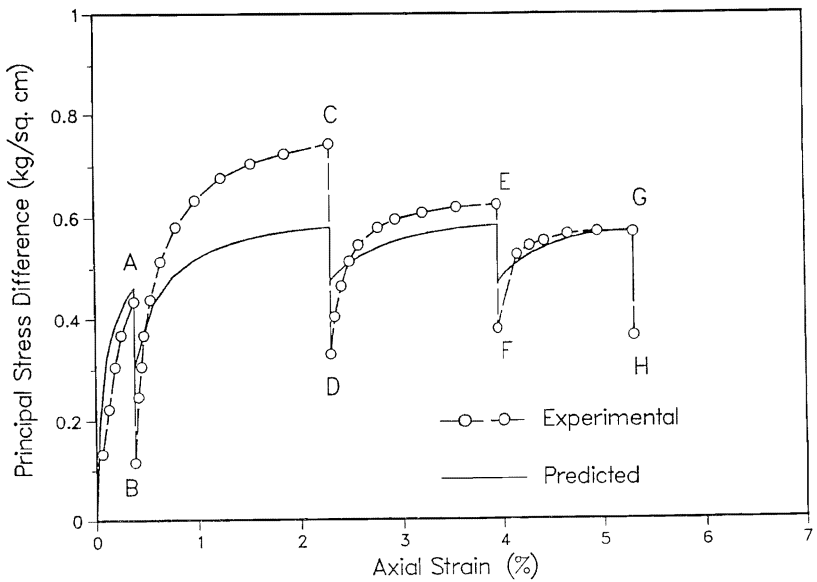

FIG. 13. Prediction of Stress Relaxation Response of San Francisco Bay Mud under Conditions of Undrained Triaxial Stress Relaxation [after Lacerda (1976)] (1 kg/cm² = 98.1 kPa)

$$\Delta\hat{\sigma} = \frac{\hat{\delta}}{r - \dfrac{r}{s_v}} = \frac{s_v}{b(s_v - 1)} - 1 \tag{50}$$

represents this "distance." The elastic domain is represented by the "elastic nucleus" (Fig. 12), which though similar to a yield surface, is not identical since (I, J) can smoothly cross its boundary at $\hat{\delta} = r/s_v$. Assuming normality